journal

J. Am. Ceram. Soc., **82** [11] 3097–104 (1999)

Subcritical Crack Growth in a Phosphate Laser Glass

Stephen N. Crichton*,† and Minoru Tomozawa*

Rensselaer Polytechnic Institute, Troy, New York 12180

Joseph S. Hayden

Schott Glass Technologies, Inc., Duryea, Pennsylvania 18642

Tayyab I. Suratwala and John H. Campbell

Lawrence Livermore National Laboratory, Livermore, California 94551

The rate of subcritical crack growth in a metaphosphate Nd-doped laser glass was measured using the double-cleavage-drilled compression (DCDC) method. The crack velocity is reported as a function of stress intensity at temperatures ranging from 296 to 573 K and in nitrogen with water vapor pressures ranging from 40 Pa (0.3 mmHg) to 4.7×10^4 Pa (355 mmHg). The measured crack velocities follow region I, II, and III behavior similar to that reported for silicate glasses. A chemical and mass-transport-limited reaction rate model explains the behavior of the data except at high temperatures and high water vapor pressures where crack tip blunting is observed. Blunting is characterized by an arrest in the crack growth followed by the inability to reinitiate slow crack growth at higher stresses. A dynamic crack tip blunting mechanism is proposed to explain the deviation from the reaction rate model.

I. Introduction

OXIDE glass under tensile stress can exhibit enhanced slow crack growth in the presence of water or water vapor. Although there is considerable debate about the exact mechanism, it is generally accepted that water vapor attacks the region around the crack tips of surface flaws, weakening the structure in the vicinity of the crack tip. This allows cracks to grow at stress intensities below the critical value (K_{Ic}) for fracture in a dry environment.

The experimental characterization of this phenomenon was first accomplished by Wiederhorn[1] on soda–lime silicate glasses. Wiederhorn used a geometry known as the double cantilever cleavage (DCC) technique (Fig. 1(a)) to measure crack velocity (v) versus stress intensity (K_I). The stress intensity was calculated analytically from the sample geometry, the applied load, and the crack length. It is important to note that with this geometry, the stress intensity increases as the crack length increases under a constant applied load, so the crack velocity is continuously accelerating throughout the measurement. Wiederhorn found that the stress intensity needed for crack growth at a certain velocity increased as the water vapor pressure decreased, a strong indication that water was necessary to weaken the structure. This observation has been confirmed many times in various mechanical test geometries and also for both gaseous and liquid water environments.

There is abundant literature on the crack growth of silicate glasses, but to our knowledge no data exist on phosphate glasses. Multicomponent phosphate glasses are important as hosts for laser ions, especially in applications where high output energy and high peak power are required.[2] These glasses are excellent laser ion hosts, but suffer from several problems. One problem is that phosphate glasses are readily attacked by water, much more so than silicate glasses. Another problem is that these glasses have significantly lower fracture toughness than silicate glasses (approximately 0.4–0.5 MPa·m$^{1/2}$ for metaphosphates[2,3] and 0.7–1.1 MPa·m$^{1/2}$ for silicates[4]).

Initially we attempted to measure slow crack growth in these glasses as a function of temperature and humidity using the DCC geometry. However, preliminary measurements proved unsuccessful. Whenever a crack formed in the specimen, it grew so rapidly that useful data could not be obtained. Therefore, a different approach was taken. An alternative geometry first proposed by Janssen[5] offered a solution. The geometry, known as the double-cleavage-drilled compression (DCDC) geometry (Fig. 1(b)), features a stress intensity that *decreases* as the cracks grow under a constant applied load. When this sample is loaded in compression, the top and bottom of the hole experience a tensile stress which, under sufficient load, leads to the formation and growth of a pair of opposing cracks. The stress intensity decreases as the crack tips move farther away from the hole, so the crack growth rate decelerates as the crack grows. Thus this geometry is more stable since the cracks are slowing down continuously. The one disadvantage of this geometry is that there is no analytical solution for calculating the stress intensity, K_I, as a function of crack length, ℓ. Janssen[5] offered a solution by finite element analysis for determining K_I. This solution was later confirmed by Michalske *et al.*,[6] who also found an empirical equation that described the stress intensity as a function of crack length for a substantial range of crack lengths. The empirical equation is accurate to within 10% of the "exact" solution offered by finite element analysis.

An important consideration in the strength of brittle materials is crack tip blunting. In the original Griffith theory,[7] the strength of a sample is reciprocally proportional to the square root of the crack length, under the assumption that all crack tips have the same sharp radius of curvature. In the years that followed, the fracture mechanics community continued to assume that all crack tips are atomistically sharp. However, there are many indications that the crack tip of glasses can be made blunt. For example, it is known that the strength of abraded glass rods increases after soaking in water. Ito and Tomozawa[8] showed that the strengthening of abraded silica glass by soaking in hot water is faster when the hot water contains silicic acid ($Si(OH)_4$), and proposed that crack tip blunting occurs by

S. W. Wiederhorn—contributing editor

Manuscript No. 189887. Received September 8, 1998; approved May 10, 1999.
*Member, American Ceramic Society.
†Now at Ferro Corporation, Cleveland, Ohio 44131.

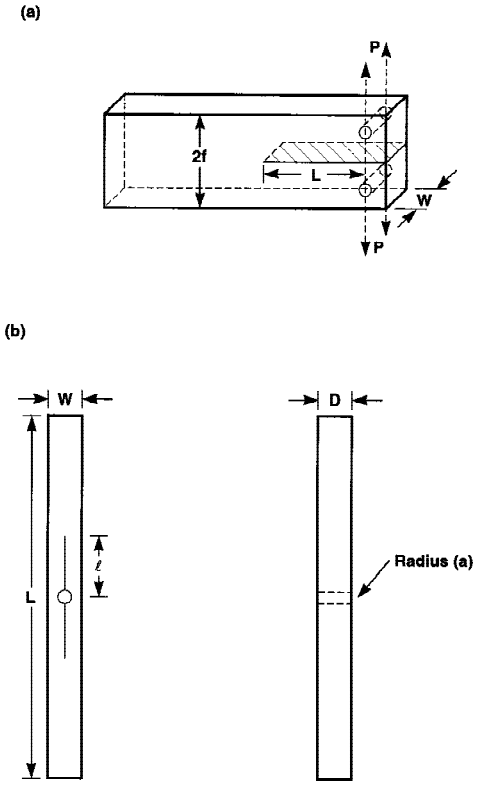

Fig. 1. Typical sample geometries used for slow crack growth measurements: (a) Wiederhorn[1] double-cantilever-cleavage (DCC) geometry, and (b) Janssen[5] double-cleavage-drilled compression (DCDC) geometry. Geometry (b) was used exclusively in these experiments.

a dissolution and reprecipitation mechanism. Lawn *et al.*[9] offered an alternative explanation for this strengthening of abraded glasses. They proposed that residual stress was created around the flaws during the abrasion process and that the residual tensile stress was released during the water soak, thus increasing the strength of the soaked samples. Later, Bando *et al.*[10] showed electron micrographic evidence for the presence of a blunt crack tip in silica glass.

Since phosphate glass is generally more susceptible to water attack than most glasses studied to date, there is a possibility that crack tip blunting occurs more readily in phosphate glasses than in silicate glasses. Also, the relatively low T_g of phosphate glasses could aid in crack tip blunting at a given temperature, especially if viscous flow is the mechanism by which blunting occurs.

In this study, the crack growth rate of the phosphate glass samples is measured and modeled as a function of temperature and humidity. Evidence for crack tip blunting is discussed.

II. Experimental Procedure

The glass used in this study (LG-770) is a multicomponent, near metaphosphate glass (O/P ~ 3). LG-770 is commercial laser glass developed by Schott Glass Technologies, Inc., that has the following approximate composition (mol%): 58–62% P_2O_5, 6–10% Al_2O_3, 20–25% K_2O, and 5–10% MgO. The glass that we used had a doping of about 4×10^{20} Nd^{3+} ions/cm^3 or about 1.8 mol% Nd_2O_3. This glass composition is typical of commercially available laser glasses used in high-peak-power fusion laser systems (see, for example, Ref. 11). T_g for this glass, measured at the onset of the DTA peak, was 742 K. The glass samples were fabricated into rectangular pieces 75 mm × 7.5 mm × 6.5 mm and a hole of 1 mm radius was core-drilled through each sample at the center of the 75 mm × 7.5 mm face of the specimen (Fig. 1(b)). The two sample surfaces containing the hole were polished prior to core drilling. This is the same geometry used by Michalske *et al.*[6] Two opposing starter cracks were cut at the top and bottom of the hole using a 0.3 mm diameter diamond-coated wire. Two stainless steel hemispheres were cut from ball bearings and secured to the top and bottom of the sample by mounting wax following the procedure employed by Helfinstine.[12] This was done to ensure that the load was distributed evenly across the cross section of the sample, as opposed to the point or line loading possible if the end faces of the sample are not perfectly flat and aligned with the compression grips.

The samples were loaded in a Model 8562 Instron, capable of both load and position control, with a 500 kg load cell. A 0.095-m-diameter × 0.14-m-long cylindrical environment chamber was constructed with temperature control to within about ±1.5 K at 296 K to about ±3 K at 673 K. The load was controllable to within ±0.1 kg, and the crosshead position to within 1 μm. The sample was loaded in compression between two flat plates by slowly bringing the plates closer to each other with the machine in position control. When a load of ~5–10 kg was reached, the machine was switched to load control, and the load was increased to 20 kg. The sample was held at this point until the temperature and water vapor pressure conditions for that particular run were achieved. Most of the runs, unless otherwise noted, were done under controlled atmosphere conditions. In humid atmospheres, the desired water vapor pressure was generated by bubbling nitrogen gas through a water bath kept at a constant temperature within ±1°C at low temperatures at ±2°C at high temperatures. Dry atmospheres were achieved by using a nitrogen gas flow of 5×10^{-7} m^3/s from a standard compressed gas cylinder either used directly or by passing through a liquid nitrogen cryogenic trap. The N_2 gas used from the compressed gas cylinder contained less than 2600 ppm H_2O by volume (manufacturer's specification) whereas the cryogenically cooled N_2 contained an estimated 395 ppm H_2O by volume.

The position of the crack tip was monitored by use of a 14× magnification cathetometer that could resolve a change in crack tip position of about 10 μm (diffraction limit). The cathetometer crosshair was initially set at the bottom of the hole and the downward growing crack was monitored relative to this starting point. The cathetometer crosshair position was controlled by a micrometer. After the temperature and humidity had equilibrated in the chamber, the load was raised to 100 kg, then raised in 10-kg increments until the crack was observed to grow. The crack was allowed to grow to at least 0.005 m in length, in order to minimize transient effects from the pre-crack and also because the crack must be at least that long before the empirical equation for the stress intensity becomes valid.[6] The initial loads necessary to observe growing cracks ranged from 150 to 270 kg, depending on temperature and humidity conditions.

When the crack reached the required minimum length, the load was raised an additional 10–20 kg and the data collection began. Initially the crack grew rapidly and data were taken in intervals as short as 15 s, noting the crack length to a precision of 10 μm, and also recording the elapsed time. As the crack growth slowed, the time interval between readings was increased proportionately. For some samples, after the crack growth rates had been measured for a given load, the load was increased and another set of data was taken on the same sample.

Figure 2 shows a typical set of results obtained from a single sample that was subjected to two successive loadings. Because of the nature of the DCDC experimental method, successive loadings result in overlapping measurements of velocity vs K_I. The data illustrate the excellent agreement between the velocity measurements vs K_I achieved with this procedure.

For some samples, crack propagation appeared to stop completely. For these samples, after the crack had been stopped for a period of time (at least 30 min), the load was increased in 10 kg increments until the crack growth started again. Usually the

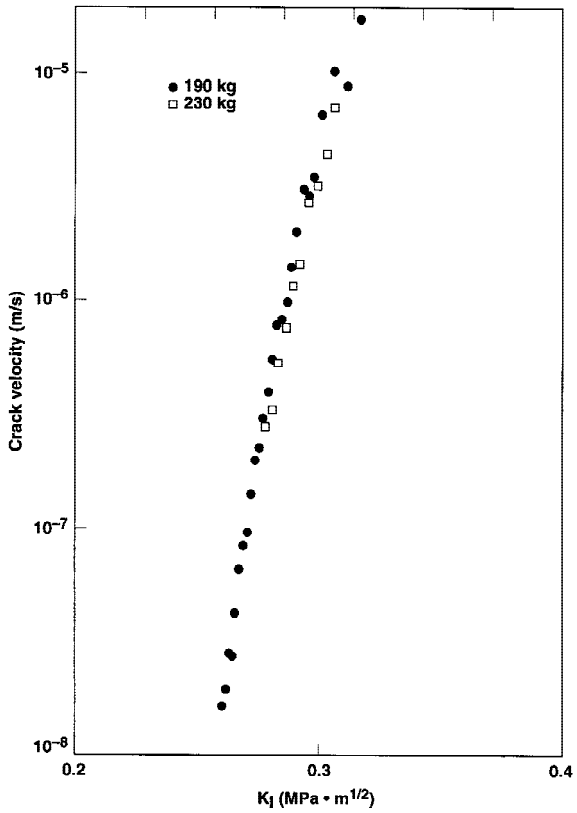

Fig. 2. Example of typical crack velocity data for phosphate glass obtained using the DCDC method and a sample subjected first to 190 and then 230 kg load (23°C, $P_{H_2O} = 2.3 \times 10^3$ Pa (17 mmHg)).

increase in load needed to restart crack growth was substantial (>30–50 kg), and in several cases, additional crack growth did not take place even when the load was raised to the 500 kg limit of the load cell. For those samples in which additional crack growth did take place, the crack grew at a rate far too fast to be observable in the experimental setup and the final length was too long to be seen through the environmental chamber viewing port.

For many samples, the cracks were observed to heal over a period of several minutes after the load was removed. The growth rate for reopening a healed crack was measured on one of these samples using the procedure described above.

The crack growth data were analyzed by plotting the measured crack velocity vs stress intensity. The stress intensity for a given crack length is given by Michalske *et al.*[6] for the sample geometry employed here:

$$K_1 = \frac{\sigma\sqrt{a}}{1.595 + 0.353\frac{\ell}{a}} \quad (1)$$

where K_I is the stress intensity (MPa·$m^{1/2}$), σ is the applied stress (MPa), ℓ is the crack length (m) measured from the center of the hole, a is the hole radius (m), and the numbers are empirically determined constants. The above equation is valid in the range of $5 < \ell/a < 12$. The crack velocity was calculated by a simple finite difference between successive data points, i.e., $v = \Delta\ell/\Delta t$ where $\Delta\ell$ is the incremental crack length for the incremental time Δt.

III. Results

(1) Dependence on Temperature and Water Vapor Pressure

Slow crack growth experiments were carried out over a range of temperatures from 296 to 573 K, water vapor pressures from 40 Pa (0.3 mmHg) to 4.7×10^4 Pa (355 mmHg) and stress intensities in the region between 0.2 to 0.4 MPa·$m^{1/2}$. The corresponding range in measured crack velocities varied from approximately 10^{-8} to 10^{-4} m/s.

The effect of temperature on crack growth rate for fixed water vapor pressures of 270 Pa (2 mmHg) and 2.3×10^3 Pa (17 mmHg) are shown in Fig. 3. In contrast, Fig. 4 plots the effect of varying water vapor pressure on crack velocity for isothermal conditions of 348, 423, and 498 K.

It is clear from the data in Figs. 3 and 4 that for a fixed stress intensity, changes in temperature have a far greater effect on crack growth velocity than do corresponding percent changes in water vapor pressure. This is expected since the velocity of crack growth is either reaction rate or diffusion limited, both of which are thermally activated processes having an exponential dependence with T^{-1}. Thus, for example, a change in temperature by 75 K can produce as much as a 10^3 to 10^4 change in crack velocity. In contrast, the effect of vapor pressure on crack velocity is more nearly linear, again in agreement with the commonly accepted chemical-reaction-driven crack growth models.

Slow crack growth of silicate glasses is generally characterized by three distinct regions[1,13] (regions I, II, and III); these three regions are also clearly seen in the experimental data on phosphate glass (Fig. 3(a)). Region I refers to the range of conditions for which crack growth is reaction-rate limited and is characterized by an approximately linear increase in the logarithm of the crack velocity vs K_I. Region II refers to the conditions over which the crack velocity appears to "plateau" to a constant value with increasing K_I. In region II the crack velocity is mass-transport limited by the rate of diffusion of

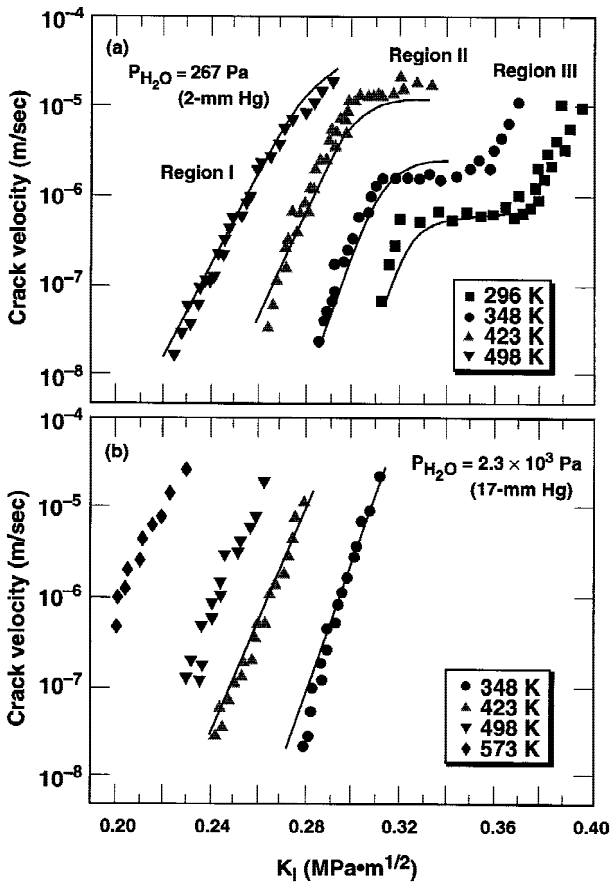

Fig. 3. Crack growth rate measured at various temperatures and constant water vapor pressures of (a) 267 Pa (2 mmHg) and (b) 2.3×10^3 Pa (17 mmHg). The lines are fits to the data using the reaction rate model (Eq. (7)) and a single set of parameters. Only those data outside the region of significant crack blunting are fitted with the model.

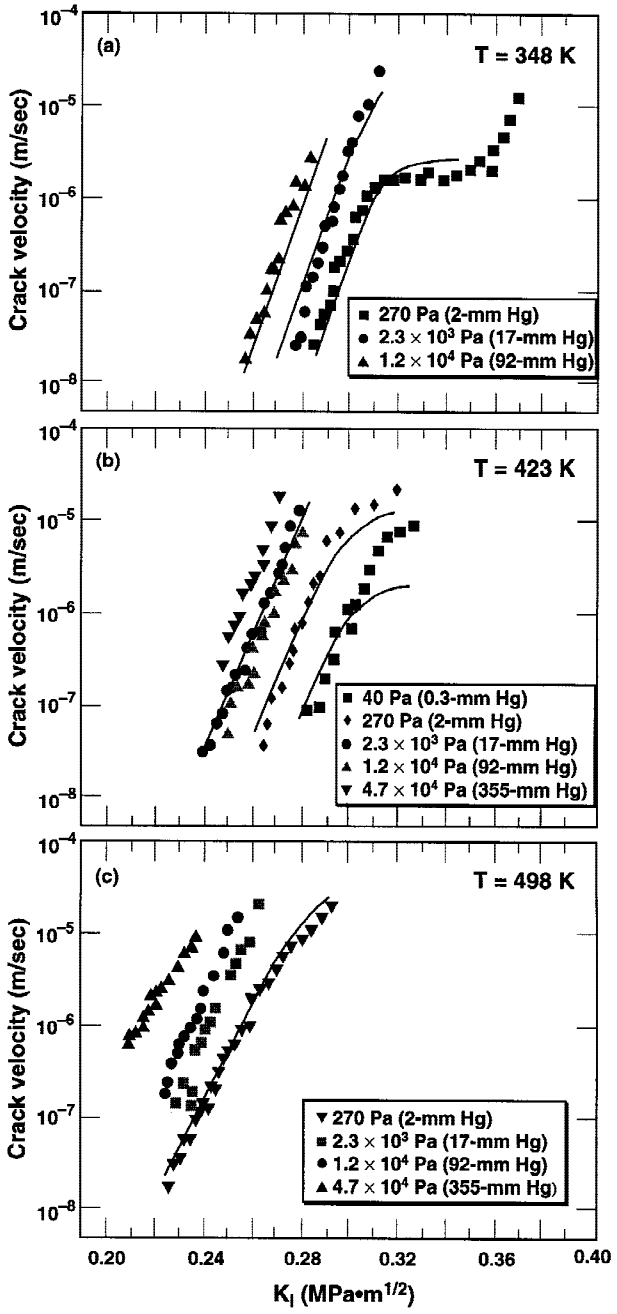

Fig. 4. Crack growth rate for various water vapor pressures at constant temperatures: (a) 348, (b) 423, and (c) 498 K. The lines represent fits to the data using the reaction rate model (Eq. (7)) and the same set of parameters used in Fig. 3. Only those data outside the region of significant crack blunting are fitted with the model.

reactants (in this case H_2O) to the crack tip; the transition from region I to region II is clearly shown in Fig. 3(a). Finally, region III refers to the conditions where crack velocity becomes independent of the chemical environment. Region III typically occurs at K_I values approaching the fracture toughness limit and is evidenced by an abrupt increase in crack velocity at the end of region II.

Under isothermal conditions the transition from region II to III in silicate glasses is typically characterized by a rapid coalescence of the various growth curves into a single band of values in which the velocity is solely a function of K_I.[1] In our study only two of the measurements extended into region III (Fig. 3(a)). However, because these measurements were carried out at different temperatures, we do not see the coalescence of crack growth curves commonly seen under isothermal conditions.

Anomalously high crack velocities were observed at 296 K at a pressure of 2.3×10^3 Pa (17 mmHg). This is illustrated in Fig. 5 which compares measured crack velocities at 296, 348, and 423 K for a fixed vapor pressure of 2.3×10^3 Pa (17 mmHg). The high crack velocities at 296 K are actually higher than those at 348 K contrary to the expected temperature dependence. The 296 K measurements are reproducible. Later we suggest a possible explanation for this anomalous behavior.

(2) Region of Crack Arrest under Load

With the DCDC crack growth method (see Section II) the stress intensity at the crack tip decreases as the crack grows and moves away from the center hole under a constant applied load. Thus the crack velocity decelerates several orders of magnitude during the course of one test. Ordinarily, the crack velocity continues to decelerate to a low, but still measurable, level. However, at high temperatures and vapor pressures, crack growth was observed to slow and then stop abruptly (at least to within detection limits). Furthermore, when the load was increased to restart the crack growth, it was found that a very large increase was necessary to re-initiate growth. Once initiated, the new crack grows too rapidly to measure and often extending beyond the range of view of the cathetometer. For a typical DCDC measurement, the test load is in the range of 200 kg; however, for two samples, increasing the load to 500 kg (the limit of the Instron load cell) still was insufficient to restart crack growth.

In this paper we refer to the failure to initiate slow crack growth upon application of a higher load as "crack tip blunting." Figure 6 shows the regions of temperature and pressure for this study where this crack blunting phenomenon is observed (defined as no measurable crack growth in ~1800 s (~30 min)). The dashed line indicates the approximately boundary of temperature and water vapor pressure conditions above which restart of crack growth becomes difficult once it has stopped. Under conditions where crack blunting is observed, the "time-to-blunt" decreases with increasing temperature and water vapor pressure. Here we define the time-to-blunt as the time difference between when crack growth has stopped under one load to the time when application of a higher load fails to reinitiate slow crack growth. Note that the observed time dependence associated with onset of blunting suggests that it is a dynamic process.

(3) Crack Healing

In a number of cases we observed that the crack closes to the point where it becomes visually undetectable a few minutes after removing the load. This suggests that the opposing faces

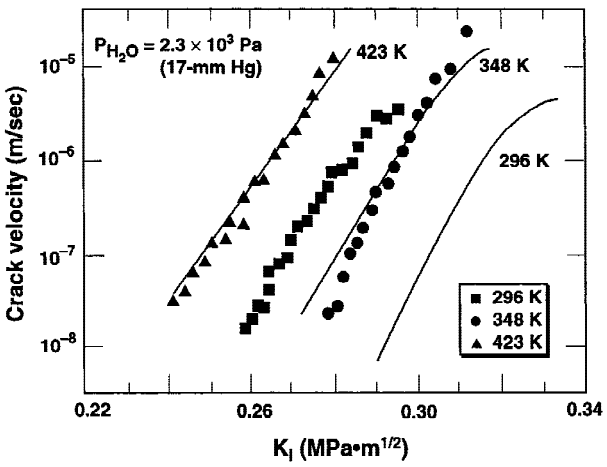

Fig. 5. Comparison of crack growth velocities measured at 296, 348, and 423 K and 2.3×10^3 Pa (17 mmHg) water vapor pressure showing the anomalous behavior at 296 K suspected to be the result of capillary condensation. The lines represent model predictions using Eq. (7).

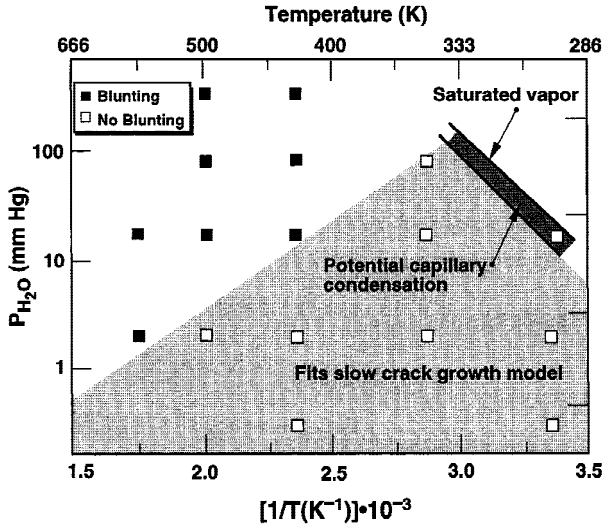

Fig. 6. Temperature and water vapor pressure regions where crack blunting is and is not significant; the dashed line is the approximate boundary between these two regions. In the region above the dashed line, crack tip blunting significantly influences crack growth whereas the region below the line shows negligible blunting and is accurately represented by the slow crack growth model (Eq. (7)). The shaded region between the two solid lines represents the P_{H_2O} vs T region of potential capillary condensation at the crack tip; the upper line is the water-saturated vapor pressure and the lower line represents the limit for capillary condensation for a crack tip radius of 1.5 nm.

may have rebonded (i.e., the crack has "healed"). To test this, one such sample was retested in the Instron. The results show that the healed crack recovered a significant portion (~80%) of the original glass strength, indicating substantial bonding between the crack faces. Wiederhorn and Townsend,[14] Stavrinidis and Holloway,[15] and Michalske and Fuller[16] observed similar crack healing behavior for cracks in silicate glasses.

IV. Discussion

As stated above, it is well known that slow crack growth measurements on silicate glasses show three characteristic regions of crack velocity versus stress intensity and the data presented here for phosphate glass show similar behavior. Although the exact chemical mechanism of crack propagation is not completely understood, it is generally accepted that the crack front movement in regions I and II involves the transport of H_2O through the crack and the subsequent reaction between water and the crack tip. Hence it is believed that the rate of crack growth is governed by a combination of reaction kinetics and mass transfer. Various models have been developed to describe crack growth in regions I and II with the most widely accepted being that of Weiderhorn.[1,17,18] In this section Wiederhorn's model is used to analyze the data over the range of conditions for which the model is valid (i.e., no change in crack tip radius). This analysis leads to two main results. First, a set of model parameters are derived that accurately predict crack growth under most experimental conditions. These model parameters can be used in engineering applications for predicting crack growth in phosphate glass over a broad range of process conditions. Second, the analysis shows that the model tends to break down at high temperature and high water vapor pressure where crack tip blunting is observed. This suggests a physical picture of the crack growth in phosphate glass in which crack propagation competes with crack blunting. This also suggests avenues of further experimental and modeling work needed to more accurately describe crack growth in phosphates.

(1) Behavior in Region I

Wiederhorn's model describes the dependence of crack growth on stress intensity, temperature, and water vapor pressure by the expression

$$v_I = A\left(\frac{p}{p_0}\right)^m \exp([K_I b - Q_I]/RT) \tag{2}$$

where v_I is the crack velocity in region I (m/s), p is the water vapor pressure (Pa), K_I is the stress intensity (Pa·m$^{1/2}$), and R and T have their usual meanings. We normalized the water vapor pressure to 1 atm (i.e., 1.013×10^5 Pa (760 mmHg)); thus p/p_0 represents the relative variation in reactant concentration. The model includes four parameters—A, m, b, and Q_I—that have various physical meanings in the reaction process: Q_I is the activation energy (kJ/mol), m is the "order" of the reaction in terms of the water vapor reactant, and A (m/s) can be likened to the preexponential constant that often appears in reaction rate expressions. The parameter b (m$^{5/2}$/mol) is related to the activation volume and is discussed in more detail later.

Values for the four model parameters ($A = 2.96 \times 10^6$ m/s, $m = 1.19$, $b = 0.496$ m$^{2.5}$/mol, and $Q_I = 216$ kJ/mol) were determined by a multiple regression analysis of the data taken in the region where crack blunting effects are negligible (see Fig. 6). The value of m was determined to be 1.19; this is close to 1.0 and suggests that crack tip bond breaking is governed by reaction kinetics first-order in H_2O. Wiederhorn's analysis of the crack growth in soda–lime silicate glass at moderate to high vapor pressures (similar to those used here) also showed $m = 1$; however, at lower vapor pressures m decreased to a value of about 0.5 in the soda–lime glass. Soga *et al.*,[19] on the other hand, observed $m = 1$ by eliminating gases other than water vapor.

The activation energy, Q_I, for crack growth in this phosphate glass is 216 kJ/mol, which is significantly greater than the value of 109 kJ/mol reported for crack growth in soda–lime glass in liquid water.[18] This partially explains the greater temperature sensitivity of crack growth in phosphate glass compared to silicates although the exact nature of the rate-controlling reaction step remains unknown.

Physical insight into the significance of the parameter, b, can be gained by equating Wiederhorn's model for crack growth with a similar equation developed by Hillig and Charles to describe crack growth at a constant water vapor pressure:[20,21]

$$v_I = A' \exp\left[\left(-Q_I + \frac{2V_a K_I}{3\sqrt{\pi\rho}}\right)/RT\right] \tag{3}$$

where A' is a preexponential constant (m/s), V_a is the activation volume (m^3/mol), and ρ is the crack tip radius (m). Equating the Weiderhorn model (Eq.(2)) with that of Hillig and Charles (Eq. (3)) shows that b is related to the activation volume and crack tip radius:

$$b = \frac{2V_a}{3\sqrt{\pi\rho}} \tag{4}$$

The value of $b = 0.496$ m$^{5/2}$/mol was determined by the regression analysis. This value is similar to the previously obtained values,[21] 0.26–0.88, for various different glasses. If we assume a crack tip radius of 1.5 nm as determined by electron micrograph for silica glass,[10] then one can use Eq. (4) to estimate an activation volume for crack growth of 51.1×10^{-6} m^3/mol for this phosphate glass. If we use a crack tip radius of 0.5 nm (characteristic of an atomically sharp crack), the value used by Wiederhorn *et al.*,[21] we get an activation volume of 29.5×10^{-6} m^3/mol.

(2) Behavior in Region II

As previously stated, the characteristic plateau region where the crack growth rate becomes nearly independent of the stress intensity is called region II. This occurs when the crack growth becomes limited by the rate at which water is transported to the crack tip.[1] The region II crack velocities follow an Arrhenius temperature dependence indicative of a thermally activated mass transport process. Based on this observation and knowing the transport rate depends linearly on the water vapor pressure,

the following expression can be used to model crack velocity (v_{II}) in region II:

$$v_{II} = C \cdot \frac{p}{p_0} \cdot \exp\left(\frac{-Q_{II}}{RT}\right) \quad (5)$$

where C is a preexponential constant (m/s), Q_{II} is the activation energy for transport (kJ/mol), and the other terms have been defined previously. The values for C and Q_{II}, determined from the present crack growth data, are 8.21 m/s and 26 kJ/mol, respectively.

The mechanism of H_2O mass transport to the crack tip has been the subject of previous investigations.[1,22] Wiederhorn[1] assumed H_2O mass transport to be controlled by gas diffusion across a boundary layer at the crack tip in his study of crack growth in soda–lime glass. He further assumed that the water concentration outside the boundary layer remained constant and was continuously replenished by the bulk flow of the surrounding humid inert gas (N_2) into the void created by the growing crack. Lawn[22] later extended Wiederhorn's gas diffusion concept to include Knudsen diffusion (molecular flow) by arguing that the mean free path between gas molecule collisions is greater than the assumed crack tip separation of 0.1 μm.

Bulk gas diffusion and Knudsen diffusion depend on temperature as T^3 and $T^{1/2}$, respectively. The crack velocity in region II is mass-transport limited and therefore dependent on the product of the diffusion coefficient and the water vapor concentration. Assuming the temperature dependence of the water vapor concentration follows the ideal gas law (T^{-1}), then the crack velocity should show a $T^{1/2}$ and $T^{-1/2}$ dependence if controlled by bulk gas and Knudsen diffusion, respectively. In contrast, the data from this study show a much steeper temperature dependence suggesting that for phosphate glasses the gas diffusion mechanisms mentioned above are not the rate-controlling step for mass transport to the crack tip.

One alternative explanation is mass transport by surface diffusion. The rate of surface diffusion is controlled by the activation energy separating adjacent adsorption sites and, therefore, would be expected to follow an Arrhenius-type temperature dependence. Morariu and Mills[23] have studied the self-diffusion of adsorbed water on hydrated silica surfaces and report an activation energy of about 20–25 kJ/mol for water in the second statistical monolayer. This is in reasonable agreement with the activation energy reported here (26 kJ/mol). Note that energies less than about 40 kJ/mol often correspond to weak bonds associated with physical absorption on a surface or hydrogen bonding.[24]

Although it is tempting to conclude that surface diffusion is the controlling mass transport process in this study, there are other plausible mechanisms. For example, bulk gas diffusion that is modified by adsorption on the crack surface[25] may also account for the observed temperature dependence. In such a case, the effective gas diffusion coefficient, D_{eff}, is expressed as[25]

$$D_{eff} = D/(1 + K_a A/V) \quad (6)$$

where K_a is an equilibrium constant describing the distribution of H_2O adsorbed on the solid surface vs that in the gas phase, and V (m^3) and A (m^2) represent the crack volume and the exposed surface area, respectively. According to Eq. (6) the adsorption of water on the crack surface has the effect of reducing the bulk diffusion rate and thus K_a is often referred to as the retardation factor. In general, the greater the degree of adsorption of water on the crack surface, the larger the overall reduction in the effective gas diffusion rate. Despite this retardation effect, the temperature dependence of K_a can cause D_{eff} to increase with temperature, particularly if K_a is an activated process.

Okamoto and Tuzi[25] have used Eq. (6) to model the adsorption of water on soda–lime and borosilicate glasses at very low water vapor pressures (~1.3×10^{-3} Pa, ~10^{-5} mmHg) and low coverage (≤1% of a monolayer) over a range of 273 to 403 K. Their data show an exponential decrease in K_a with increased temperature (i.e., D_{eff} increases exponentially) with an activation energy of 29 kJ/mol. This exponential dependence is similar to what we report here.

Unfortunately, it is not possible to define the exact mechanism that controls the rate of mass transport in these experiments. Therefore, to avoid further belaboring the issue, we simply conclude that our data show an Arrhenius-type temperature dependence that is not consistent with either bulk gas diffusion or molecular flow mechanisms. Surface diffusion is one possible explanation for this behavior although other mechanisms are also plausible. Nevertheless, Eq. (5), which has been empirically derived from our data, can be used to accurately predict region II crack velocities over the range of temperature and pressure conditions reported here.

The expressions for v_I and v_{II} (i.e., Eqs. (2) and (5)) describe the crack growth velocity in the limits of regions I and II, respectively. These two velocities can be combined into a single expression describing the composite slow crack growth velocity across both regions I and II.

$$v = \frac{v_I v_{II}}{v_I + v_{II}} \quad (7)$$

where the composite crack growth velocity (v) is the well-known harmonic mean of the crack velocity, v_I, in region I (Eq. (2)) and, v_{II} in region II (Eq. (5)). Lawn[22] has used a similar approach for describing the combined crack velocities of regions I and II. Note that in the limit of region I, Eq. (7) approaches $v \sim v_I$, and similarly in region II, $v \sim v_{II}$.

The velocities calculated by Eq. (7) are compared to the experimental data in Figs. 3–5. Good agreement of the model with the data were obtained for temperatures and vapor pressures where crack tip blunting is negligible. In Section IV(4) we discuss the effects of blunting on the model predictions.

(3) Crack Growth Enhanced by Capillary Condensation

One possible explanation for the anomalous behavior of the crack growth at 296 K and 2.3×10^3 Pa (17 mmHg) is capillary condensation at the crack tip. Under such conditions the measured crack growth would tend to approach a growth rate expected in liquid water rather than in water vapor. The possibility of water condensation at the crack tip has been proposed by others, particularly for conditions in which the relative humidity exceeds 30%.[1] In addition, the presence of any glass corrosion products in the water phase would further reduce the equilibrium vapor pressure.

Capillary condensation implies a state of localized thermodynamic equilibrium between a liquid and vapor phase. Such conditions can exist even at a moving crack front as long as the rate of mass transport of water vapor to the crack tip exceeds the combined rate of crack tip motion and water consumption associated with bond breaking during fracture growth. Region I is the region of chemical-kinetic limited growth and therefore meets this requirement.

Capillary condensation is described by the well-known Kelvin equation, which relates the curvature of a surface to the associated equilibrium vapor pressure. For the present case of a line crack,

$$\frac{p_r}{p_s} = \exp\left(\frac{\gamma M}{rdRT}\right) \quad (8)$$

where p_r is the equilibrium vapor pressure (Pa) above a curved liquid surface of radius r (m), molecular weight M (kg/mol), density d (kg/m^3) and having surface tension γ (J/m^2); p_s is the equilibrium saturation vapor pressure (Pa) above a flat surface.

The vapor pressure reduction (i.e., p_r/p_s) for water at a crack tip at 296 K is estimated to be about 0.5 (50% relative humidity). Here we assume a crack tip radius of 1.5 nm as reported by Bando *et al.*[10] based on TEM measurements of a crack in silica glass. The pressure reduction is more than sufficient to

lead to capillary condensation at the crack tip when using a water vapor pressure of 2.3×10^3 Pa (17 mmHg) at 296 K; the saturation pressure at this temperature is 2.8×10^3 Pa (21 mmHg), giving p/p_s of 0.83 (83% relative humidity). It is possible that this capillary condensation is the cause of the greater crack growth rate at this temperature.

In Fig. 6 we include the water saturation pressure (i.e., 100% relative humidity) versus temperature and also the corresponding vapor pressure estimated for the onset of capillary condensation at the crack tip. Our experimental condition of 296 K and 2.3×10^3 Pa (17 mmHg) falls within these two limits.

Alternately, the anomalous crack growth of the present glass at low temperature may be due to the nature of the phosphate glass surface which collects water from the atmosphere. Recent experiments by one of the authors indicate that the surface of this phosphate glass undergoes unusual reaction with water.[26]

(4) Crack Tip Blunting

The difficulty of reinitiating crack growth at high temperatures and water vapor pressures can be interpreted as an effective increase in the crack tip radius; in other words, the tip becomes blunt. As noted earlier, an alternative explanation of residual stress release was suggested[9] for the similar strength increase. But in the present experiment no residual stress is involved. We use this crack tip blunting, i.e., change of crack tip radius, without change of crack length to analyze the results from our experiments.

The approximate temperature and pressure conditions where crack blunting becomes significant are shown in Fig. 6; the dashed line roughly separates the regions of significant vs negligible blunting. These data are for a holding time of ~1800 s (~30 min); the line would be shifted lower for longer holding times. In view of the large viscosity-reduction effect of water in glass, it is plausible that the blunting mechanism is glass viscous flow promoted by water entry into the glass from the atmosphere.

As noted above, we make the assumption that crack tip blunting is due to an effective change in radius of the crack tip. Therefore, we can estimate the relative change in the crack tip radius due to blunting from the relative increase in load needed to restart crack growth:

$$\frac{\rho_b}{\rho_0} = \left(\frac{\sigma_b}{\sigma_0}\right)^2 \tag{9}$$

where ρ_0 and ρ_b are the initial and blunted crack tip radii, respectively, and σ_0 and σ_b are the corresponding preblunting and postblunting loads (Pa). In some cases we found that the load needed to reinitiate crack growth was as much as 2 to 3 times the initial load, suggesting that during blunting the effective crack tip radius increased by as much as 4 to 9 times. This large increase in load necessary to reinitiate a sharp crack also explains why it then grows so quickly. The stress intensity at this new sharp crack tip would likely exceed K_{Ic} and thus rapid crack growth would be expected.

It is clear from the observed temporal dependence of the blunting process that some small change in the effective crack tip radius may occur even during crack propagation. This could explain why the standard crack growth model (Eq. (2)) fails to accurately predict crack propagation in the region where blunting was observed (Fig. 6). To test this hypothesis we used Eq. (2) and the previously determined values of A, Q, and m to fit the crack velocity data in the region where the blunting was observed; however, we used b as an adjustable parameter. Recall that b is related to the square root of the crack tip radius (Eq. (4)). Therefore, under the assumption that the activation volume (V_a) for the crack growth process is independent of crack tip radius, then any change in b reflects a corresponding change in the crack tip radius. Figure 7 shows the results of such an analysis using the crack velocity data measured at 4.7×10^4 Pa (355 mmHg) and 498 K. The solid lines represent the model predictions using Eq. (2) and with $b = 0.496$ m$^{5/2}$/mol as determined from measurements made where there is no measurable blunting (see Fig. 6). As expected the model does not accurately predict the behavior at 498 K and 4.7×10^4 Pa (355 mmHg) (i.e., the blunting region) but is in good agreement at 270 Pa (2 mmHg) (i.e., the nonblunting region). If b is reduced to 0.470 m$^{5/2}$/mol, then Eq. (2) accurately fits the data at 4.7×10^4 Pa (355 mmHg). This change represents an increase in the effective crack radius by about 11%. Similar fits to other crack velocity data taken in the blunting region all show an increase in the effective crack tip radius ranging from about 6% to 15%. Note that the magnitude of the change in the crack tip radius observed under dynamic conditions is far less than that observed when the crack is stopped. This is not unexpected because under dynamic conditions the rate of crack blunting is always competing with crack propagation. Nevertheless, as this analysis showed, even very minor changes in the effective crack tip radius produce a significant change in the rate of crack growth because of the exponential dependence of crack velocity on $\rho^{-1/2}$ (see Eq. (3)). It has been suggested[20] that the static fatigue limit often observed in soda–lime glasses represents the condition where the rate of blunting balances the rate of crack growth. This reasoning leads to the logical extension that the highest static fatigue limit is expected under conditions for the greatest rate of blunting.

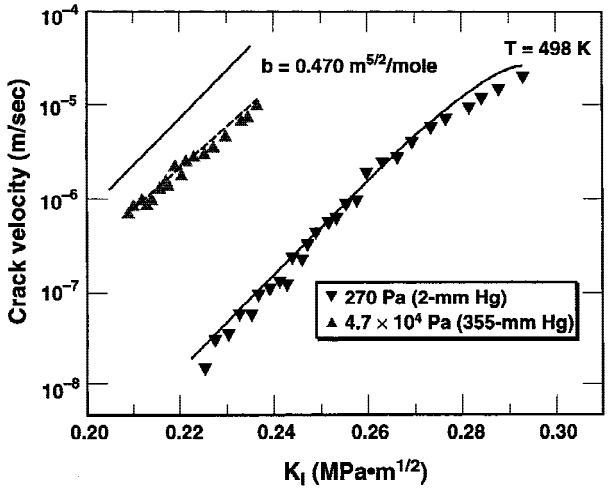

Fig. 7. Comparison of crack growth velocities measured at 267 Pa (2 mmHg) and 4.7×10^4 Pa (355 mmHg) and at 498 K. The solid lines represent the predicted behavior using Eq. (7) and $b = 0.496$ m$^{5/2}$/mol. The dashed line also uses Eq. (7) but b is reduced to 0.470 m$^{5/2}$/mol to fit the data.

One could also argue that the activation energy, Q_I (see Eq. (3)), is changing in the blunting region, not the crack tip radius. Reducing the activation energy by the same relative amount as was done for b, would achieve the same quality of fit to the data shown in Fig. 7. However, this alternate explanation requires that a change in crack tip radius occurs only when crack propagation stops completely.

Crack blunting involving mass transport to the crack tip could occur by evaporation and condensation, surface diffusion, bulk diffusion, and/or viscous flow. In the case of mass transport by viscous flow, the range of change of the radius of the crack tip is inversely proportional to the viscosity of the glass in that region. In view of the large viscosity-reduction effect of water in glass, it is likely that the operating blunting mechanism is the viscous flow promoted by water entry into the glass from the atmosphere. A more detailed study of the kinetics and mechanism of crack blunting is currently under way.

(5) Slow Crack Growth In Phosphate vs Silicate Glass

Figure 8 compares our measured slow crack growth rates in a phosphate glass at 296 K and ~10% relative humidity with

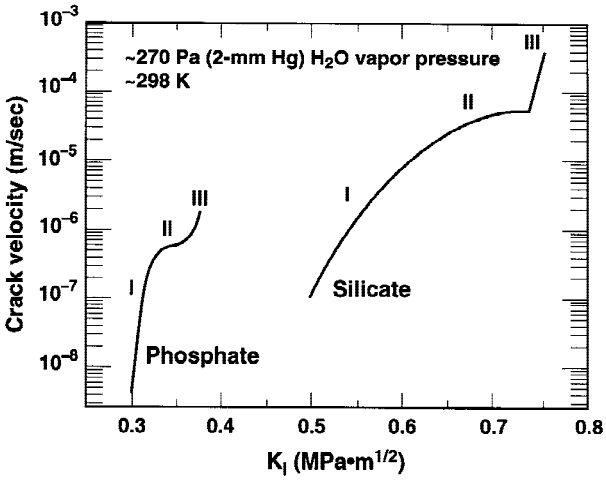

Fig. 8. Comparison of crack growth velocity measurement for phosphate glass (this study) and soda–lime silicate glass[1] at 296 K and approximately 267 Pa (2 mmHg) water vapor pressure.

corresponding data for a soda–lime silicate glass.[1] In both cases the measurements extend over regions I, II, and III.

A number of interesting differences in slow crack growth behavior of the two glasses are immediately noticeable. First, and not surprising, the phosphate glass is significantly weaker than the silicate as indicated by the much lower stress intensity values needed to reach the same crack growth velocities. Also note that in region I, the slope of the crack velocity profile for the phosphate is much greater than that of the silicate. Thus, small increases in the stress intensity for the phosphate glass cause a greater increase in crack velocity compared to that for the silicate glass.

The onset of region II occurs at a crack velocity about 10^2 lower for phosphates than for silicates. Since it is proposed that region II crack growth is controlled by diffusion of H_2O to the crack tip modified by the adsorption, then this suggests that mass transfer rates are about 10^2 slower in phosphates than silicates. The naturally higher affinity of phosphates for water compared to silicates may explain this large difference in diffusion rates. In other words, the stronger attraction of the water at the surface of the phosphate may tend to retard water transport to the crack tip; this process was discussed briefly in Section IV(2) (see Eq. (6)).

The onset of region III occurs as the stress intensity approaches the fracture toughness of the glass, i.e., about 0.45 MPa·m$^{1/2}$ for phosphate compared to approximately 0.8 MPa·m$^{1/2}$ for the soda–lime silicate. The onset of region III is much harder to measure using the DCDC method because the stress intensity (and hence growth rate) is greatest at the beginning of the measurement. Therefore, the measured transition from region II to region III behavior shown in Fig. 8 for the phosphate is probably only accurate to within stress intensity values ±0.02 MPa·m$^{1/2}$.

V. Conclusions

Crack growth velocities are reported for a phosphate laser glass over a range of temperatures and water vapor pressures. Wiederhorn's classic chemical and mass-transport-limited reaction rate model is used to explain crack growth behavior in regions I and II except when there is blunting. The results indicate that in region I the crack growth velocity varies approximately linearly with water concentration and has an activation energy, Q_I, of 216 kJ/mol. In region II the crack velocity also exhibits a linear dependence on water vapor pressure and an Arrhenius temperature dependence but the activation energy, Q_{II}, is only 26 kJ/mol. A set of model parameters are developed which can be used by glass process engineers to accurately predict the rate of slow crack growth in phosphate laser glasses over a wide range of operating environmental conditions. Blunting is interpreted as an increase in the effective radius of curvature of the crack tip. Our results suggest that under dynamic conditions, the effective crack tip radius may increase by about 10%. Under static conditions (growth arrest), the crack tip radius increases by about 4 to 9 times. Anomalous crack growth near the point of water saturation at 296 K is discussed in terms of possible capillary condensation at the crack tip.

Acknowledgments: We gratefully acknowledge the assistance of the late Mr. William A. "Bill" Steele in the construction of the environmental chamber and fabrication of the glass samples used in this study. This research was funded by the U.S. Department of Energy by Lawrence Livermore National Laboratory under Contract No. W-7405-Eng-48.

References

[1]S. M. Wiederhorn, "Influence of Water Vapor on Crack Propagation in Soda–Lime Glass," *J. Am. Ceram. Soc.*, **50** [8] 407–14 (1967).
[2]J. H. Campbell, "Recent Advances in Phosphate Laser Glasses for High Power Applications"; pp. 3–39 in Critical Reviews of Optical Science and Technology, Vol. CR64, *Inorganic Optical Materials.* Edited by P. Klocek. SPIE—The International Society for Optical Engineering, Bellingham, WA, 1996.
[3]J. E. Marion, "Fracture of Solid State Laser Slabs," *J. Appl. Phys.*, **60** [1] 69–77 (1986).
[4]J. Mencík, "Fracture Toughness of Glass and Ceramics"; pp. 119–22 in *Strength and Fracture of Glass and Ceramics.* Elsevier, New York, 1992.
[5]Ch. Janssen, "Specimen for Fracture Mechanics Studies on Glass"; pp. 23–30 in Proceedings of the 10th International Congress on Glass, Vol. 10. Ceramic Society of Japan, Tokyo, Japan, 1974.
[6]T. A. Michalske, W. L. Smith, and E. P. Chen, "Stress Intensity Calibration for the Double Cleavage Drilled Compression Specimen," *Eng. Fract. Mech.*, **45** [5] 637–42 (1993).
[7]A. A. Griffith, "Theory of Rupture," *Philos. Trans. R. Soc. London*, **A221**, 163–98 (1920).
[8]S. Ito and M. Tomozawa, "Crack Blunting of High Silica Glass," *J. Am. Ceram. Soc.*, **65** [8] 368–71 (1982).
[9]B. R. Lawn, K. Jakus, and A. C. Gonzalez, "Sharp vs. Blunt Crack Hypothesis in the Strength of Glass: A Critical Study Using Indentation Flaws," *J. Am. Ceram. Soc.*, **68** [1] 25–34 (1985).
[10]Y. Bando, S. Ito, and M. Tomozawa, "Direct Observation of Crack Tip Geometry of SiO_2 Glass by High-Resolution Electron Microscopy," *J. Am. Ceram. Soc.*, **67** [3] C-36–C-37 (1984).
[11]Y. T. Hayden, S. A. Payne, J. S. Hayden, J. H. Campbell, M. K. Aston, and M. L. Elder, "Phosphate Glass Useful in High Energy Lasers," U.S. Pat. No. 5 526 369, June 11, 1996.
[12]J. D. Helfinstine, S. T. Gulati, and D. G. Pickels, "Slow Crack Growth in High Silica Glasses"; pp. 654–58 in *The Physics of Non-Crystalline Solids.* Edited by L. D. Pye, W. C. LaCourse, and H. J. Stevens. Taylor and Francis, London, U.K., 1992.
[13]S. W. Frieman, "Fracture Mechanics of Glass"; pp. 21–78 in *Glass Science and Technology*, Vol. 5, *Elasticity and Strength in Glasses.* Edited by D. R. Uhlmann and N. J. Kreidl. Academic Press, New York, 1980.
[14]S. M. Wiederhorn and P. R. Townsend, "Crack Healing in Glass," *J. Am. Ceram. Soc.*, **53** [9] 486–89 (1970).
[15]B. Stavrinidis and D. G. Holloway, "Crack Healing in Glass," *Phys. Chem. Glasses*, **24** [1] 19–25 (1983).
[16]T. A. Michalske and E. R. Fuller, Jr., "Closure and Repropagation of Healed Cracks in Silicate Glass," *J. Am. Ceram. Soc.*, **68** [11] 586–90 (1985).
[17]S. M. Wiederhorn, "Chemical Interaction of Static Fatigue," *J. Am. Ceram. Soc.*, **55** [2] 81–85 (1971).
[18]S. M. Wiederhorn and C. H. Bolz, "Stress Corrosion and Static Fatigue of Glass," *J. Am. Ceram. Soc.*, **53** [10] 543–48 (1970).
[19]N. Soga, T. Okamoto, T. Hanada, and M. Kunugi, "Chemical Reaction Between Water Vapor and Stressed Glass," *J. Am. Ceram. Soc.*, **62** [5–6] 309–10 (1979).
[20]W. B. Hillig and R. J. Charles, "Surfaces, Stress-Dependent Surface Reactions, and Strength"; pp. 682–705 in *High Strength Materials.* Edited by V. F. Zackay. Wiley, New York, 1965.
[21]S. M. Wiederhorn, H. Johnson, A. M. Diness, and A. H., Heuer, "Fracture of Glass in Vacuum," *J. Am. Ceram. Soc.*, **57** [8] 336–41 (1974).
[22]B. R. Lawn, "Diffusion-Controlled Subcritical Crack Growth in the Presence of a Dilute Gas Environment," *Mater. Sci. Eng.*, **13** [3] 277–83 (1974).
[23]V. V. Morariu and R. Mills, "Self-Diffusion of Water Adsorbed on Silica," *Z. Phys. Chem. Neue Folge*, **79** [1/2] 1–9 (1972).
[24]A. W. Adamson, "Adsorption of Gases and Vapors on Solids"; pp. 517–600 in *Physical Chemistry of Surfaces.* Wiley Interscience, New York, 1982.
[25]H. Okamoto and Y. Tuzi, "Adsorption of Water Vapor on Glass and Other Materials in Vacuum," *J. Phys. Soc. Jpn.*, **13** [6] 649–55 (1958).
[26]Y.-K. Lee and M. Tomozawa, "Effect of Water Content in Phosphate Glasses on Slow Crack Growth Rate," *J. Non-Cryst. Solids*, **248**, 203–10 (1999). □